Journal of Materials Chemistry B

RSC Publishing

COMMUNICATION

View Article Online
View Journal | View Issue

Building triangular nanoprisms from the bottom-up: a polyelectrolyte micellar approach

Cite this: *J. Mater. Chem. B*, 2013, **1**, 4212

Received 30th May 2013
Accepted 10th July 2013

DOI: 10.1039/c3tb20765j

www.rsc.org/MaterialsB

Weiwei Ding,[a] Jiaping Lin,*[a] Kejian Yao,[a] Jimmy W. Mays,[bc] Muruganathan Ramanathan[d] and Kunlun Hong*[d]

Charge-regulated synthesis of triangular prisms in aqueous solution using self-assembled polyelectrolyte micelles as templates is described in detail. Micelles formed from amphiphilic polystyrene-*block*-sulfonated poly(1,3-cyclohexadiene) (PS-*b*-sPCHD) serve as templates to direct the formation of novel triangular prisms of $CuCl_2$ single crystals. We demonstrate that the edge lengths of these triangular prisms can be easily tailored at room temperature from the nanoscale to the mesoscale by simply adjusting the ratio of charged micelles to protons in the solution. This approach can be extended to the preparation of different ordered crystal structures with a precision hard to achieve *via* other approaches.

Among various shapes of nanoparticles, inorganic triangular nanoprisms have garnered significant research interest owing to their unique optical and conductive properties such as strong plasmon bands in the visible and IR regions, anisotropic electrical conductivity, *etc.*[1] The triangular nanoprisms (also referred to as nanotriangles, triangular nanoplates or triangular nanoparticles), with their shape-dependent property enhancement, can be used in a wide range of practical applications including biomedical imaging, cancer treatment in hyperthermia, optoelectronics, photonics, information storage, and so on.[2] Methods for fabrication of triangular nanoprisms include both bottom-up and top-down strategies. One remarkable difference between these two synthetic approaches is that the nanoprisms fabricated by top-down methods, such as lithography, are polycrystalline in nature, whereas the bottom-up synthesis, such as solution-based synthesis, leads to almost atomically flat single crystalline nanoprisms.[3]

In the bottom-up process many synthetic routes such as photo/thermal, hard or soft template approaches have been applied to synthesize nanoprisms.[1] The common attributes of shape-controlled solution synthesis involve the reduction of salt precursors or thermal/photochemical decomposition of organometallic compounds in the presence of steric stabilizers or capping agents like organic surfactants such as cetyl trimethylammonium bromide (CTAB), or polymers such as poly(vinyl pyrrolidone) (PVP).[4] Often the size, shape and size distribution of nanoprisms are controlled by adjusting the conditions of thermal treatment, irradiation wavelengths, solution pH, and the ratio of seed and capping agent. Herein, we present a new soft template route that yields triangular nanoprisms with a unimodal size distribution in addition to an exceptional control over the edge length. The approach that we present here is based on a charge regulated synthesis method in aqueous solution using amphiphilic polyelectrolyte micelles as templates. Importantly, the method allows one to deliberately tailor the edge lengths of the triangular prisms from the nanoscale to the mesoscale, at room temperature, by simply adjusting the ratio of charged micelles to protons in the solution.

In earlier studies, Koetz and others have used polyelectrolytes as reducing as well as stabilizing agents in surfactant stabilized mini/microemulsion templates.[5–7] The polyelectrolyte modified, surfactant stabilized microemulsions were successfully used as a template to control the size and shape of the nanoparticles during the formation process. For instance, the cationic polyelectrolyte poly(diallyldimethylammonium chloride) (PDADMAC) incorporated microemulsion droplets were used as reactors for the synthesis of $BaSO_4$ nanoparticles with different shapes and sizes.[8] The methodology that we present here significantly differs from the ones that have been previously reported. In our approach, an amphiphilic diblock copolymer that self-assembles into micellar structures is used as a structure directing agent where the size and shape of the nanoparticles are dictated by the

[a]*Shanghai Key Laboratory of Advanced Polymeric Materials, Key Laboratory for Ultrafine Materials of Ministry of Education, State Key Laboratory of Bioreactor Engineering, School of Materials Science and Engineering, East China University of Science and Technology, Shanghai 200237, China. E-mail: jlin@ecust.edu.cn; Tel: +86-21-64253370*

[b]*Department of Chemistry, The University of Tennessee, Knoxville, TN 37996, USA*

[c]*Chemical Sciences Division, Oak Ridge National Laboratory, Oak Ridge, TN 37831, USA*

[d]*Center for Nanophase Materials Sciences, Oak Ridge National Laboratory, Oak Ridge, TN 37831, USA. E-mail: hongkq@ornl.gov; Fax: +1-865-574-1753; Tel: +1-865-574-4974*

competing ionic interactions and the confinement effects of the polymeric micelles.

In this work, well-defined polyelectrolyte micelles formed in aqueous solution using the amphiphilic polystyrene-*block*-sulfonated poly(1,3-cyclohexadiene) (PS-*b*-sPCHD) block copolymer (BCP M_w: 15.5 kg mol^{-1}, PDI: 1.04) in which the hydrophobic PS block forms the core of the micelle while the hydrophilic sPCHD (acid form) block forms the corona. The micelles are spherical in shape with diameters ranging from 30 to 60 nm as shown in our previous paper.[9] These micelles may be used under proper conditions as templates to direct the formation of novel triangular prisms of $CuCl_2$ single crystals. It is also noteworthy that despite their unique properties[10] (super-elasticity, high electrical conductivity, *etc.*) and wide range of applications[11,12] (for instance, in solid-oxide fuel cells, gas sensors, catalysts, *etc.*) there are no simple, reproducible template-based synthetic routes currently available for creating copper chloride based nanocrystals. This article appears to be the first report in the literature of well-controlled, template-based solution synthesis of copper(II) triangles.

In a typical experiment, a simple, rational mixing of aqueous solutions of $CuCl_2$, HCl and PS-*b*-sPCHD micelles at room temperature has led to the formation of triangular prisms, as schematically shown in Fig. 1. In order to demonstrate the underlying mechanism of this process, we have judiciously varied the experimental parameters such as presence/absence of polymer micelles, micellar concentrations, PS-*b*-sPCHD polymers *vs.* unimers, and proton concentration in the solution, as discussed below.

When an aqueous $CuCl_2$ solution ($[Cu^{2+}] = 38$ mM) without any additive is dripped onto a carbon film coated nickel substrate, small spherical crystals with an average diameter of about 20 nm are formed. The introduction of hydrochloric acid (HCl) into this $CuCl_2$ solution has no observable effect on either the size or shape of the crystals. However, when 0.5 mL of PS-*b*-sPCHD micelles (final concentration of the micelles is 0.30 g L^{-1}) is added to 5 mL aqueous $CuCl_2$ solution (with $[Cu^{2+}] =$ 38 mM) and finally diluted to 10 mL, particles with rough surfaces are formed. These particles are larger than both the micelles (30–60 nm, see ref. 9) and $CuCl_2$ particles formed in the absence of micelles, as shown in the transmission electron microscopy (TEM) images (Fig. 2a). Elemental analysis by energy-dispersive X-ray (EDX) reveals that Cu and Cl are the main elements in the aggregates. The ring structures in the selected area electron diffraction (SAED) patterns indicate the formation of polycrystalline aggregates (Fig. 2e). When a small amount of acid (3.5 mM [H^+], either HCl or H_2SO_4) is added, spherical aggregates with typical polycrystalline characteristics are dominant, but a few anisotropic structures with rough surfaces (Fig. 2b) appear, indicating a so-called mesocrystalline structure.[13–16] Upon further increase of the acid concentration (6.0 mM), dramatic changes in the morphology as well as the crystal structure are observed. Triangular aggregates with rough surfaces start to form (Fig. 2c). When the H^+ concentration is further increased to 18.0 mM, uniform triangular prisms with well-defined facets and smooth surfaces are obtained (Fig. 2d). The SAED patterns shown in Fig. 2e–h clearly demonstrate the structural transitions of the aggregates from polycrystalline to a single crystalline (Fig. 2h).

To determine the structure of the observed triangular prisms, scanning electron microscopy (SEM) and high-resolution transmission electron microscopy (HRTEM) were used for further characterization. Fig. 3a shows the SEM image of the particles produced in the presence of PS-*b*-sPCHD micelles with 18.0 mM H^+ clearly indicating a three-dimensional triangular plate structure. The EDX profile demonstrates strong peaks of Cu and Cl (Fig. 3b). The HRTEM image of a triangular facet (Fig. 3c) shows visible lattice fringes, which is characteristic of a single crystal with a *d* spacing around ~1.8 Å. In addition, the

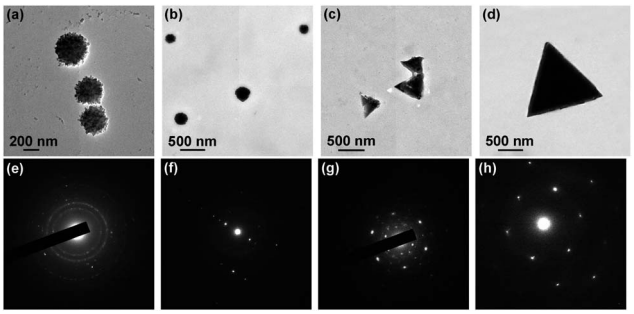

Fig. 2 TEM images (top) and the respective SAED patterns (bottom) of $CuCl_2$ particles prepared from mixed solutions having micelle concentrations of 0.30 g L^{-1}, Cu^{2+} concentration of 38.0 mM, and added H^+ concentrations of: (a) 0; (b) 3.5 mM; (c) 6.0 mM; (d) 18.0 mM.

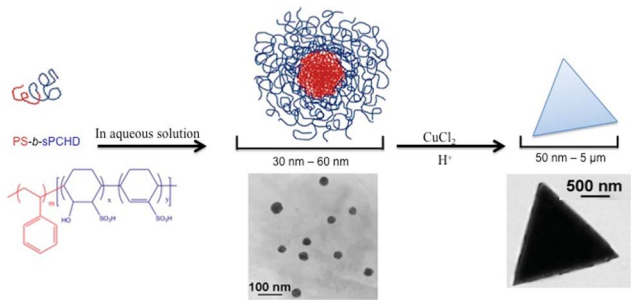

Fig. 1 Figurative description of the polyelectrolyte micelle templated synthesis of triangular copper(II) chloride prisms. The top images are schematic representations of experimentally obtained structures as shown experimentally at the bottom. The left-most figure shows the molecular scheme of the PS-*b*-sPCHD block copolymer (BCP), the middle figure shows the micellar assembly of the BCP, and the right-most figure shows the triangular prism obtained by rational mixing of copper(II) chloride, protons and polyelectrolyte micellar solutions.

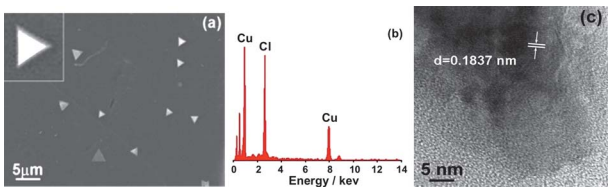

Fig. 3 (a) SEM image, (b) EDX spectrum and (c) HRTEM image of $CuCl_2$ triangular prism prepared from mixed solutions: [micelle] = 0.30 g L^{-1}, [H^+] = 18.0 mM, and [Cu^{2+}] = 38.0 mM.

SAED pattern recorded by directing the electron beam perpendicular to the triangular planar surface of an individual plate shows a typical 6-fold symmetry character (see Fig. 2h). These results also indicate that these triangular plates are single crystals with the triangular faces bound by [111] planes.

To understand the role of the charged sPCHD block in mediating $CuCl_2$ crystal growth, a series of control experiments were carried out. When PS-*b*-sPCHD micelle solution is replaced with PS-*b*-sPCHD unimers with the same Cu^{2+} and polymer ratio, two populations of particles are observed as shown in Fig. 4a. The small spherical particles are about tens of nanometers in size, which is similar to the results from $CuCl_2$ without any additive (similar to the one shown in Fig. 5a). The larger particles in Fig. 4a are irregular polygons hundreds of nanometers in size. These results indicate that there is no control over the growth of $CuCl_2$ crystalline aggregates in the presence of PS-*b*-sPCHD unimers: the growth is either unaffected (smaller aggregates) or too fast (larger aggregates). On the other hand, when sPCHD homopolymer aqueous solution is used, only semicircular shape and rod-like aggregates are formed (Fig. 4b). In both cases, the polyelectrolyte block exists as "free" chains, and the regular triangular single crystals are not observed. These results illustrate that: (1) charged polyelectrolyte blocks accelerate the $CuCl_2$ crystalline aggregation and (2) the micellar form of the charged block plays a critical role in controlling the shape of crystalline growth.

In order to further elucidate the role of micelles in the directional growth of $CuCl_2$ crystals, the effect of micelle concentration was studied. In the absence of any additive, small spherical crystals with an average diameter of about 15 nm are formed, as shown in Fig. 5a. However, the morphology of the aggregates shows a distinct dependence on the micelle concentration (Fig. 5b–d) at a given H^+ concentration (18.0 mM). The micelle and H^+ concentrations have the opposite effect on the crystalline growth. The addition of certain amounts of PS-*b*-sPCHD micelles leads to the formation of triangular plates with a well-defined single crystal structure (0.49 g L^{-1} in this case and 0.30 g L^{-1} in Fig. 2). A further increase in the micelle concentration leads to a progressive morphology change of the aggregates from the ordered triangular nanocrystal (Fig. 5b) to irregular aggregates to spherical micellar aggregates with rough surfaces (Fig. 5c and d). Such large aggregates are probably composites of $CuCl_2$ and PS-*b*-sPCHD copolymers. Thus, the equilibrations of $-SO_3H$ groups

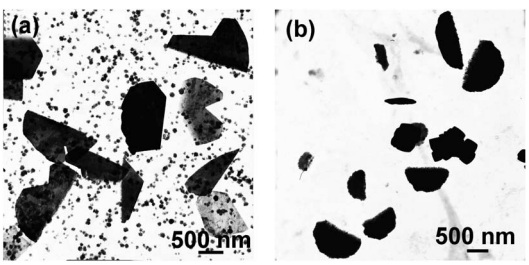

Fig. 4 TEM pictures of $CuCl_2$ crystalline aggregates prepared using (a) PS-*b*-sPCHD unimer solution; (b) sPCHD aqueous solutions.

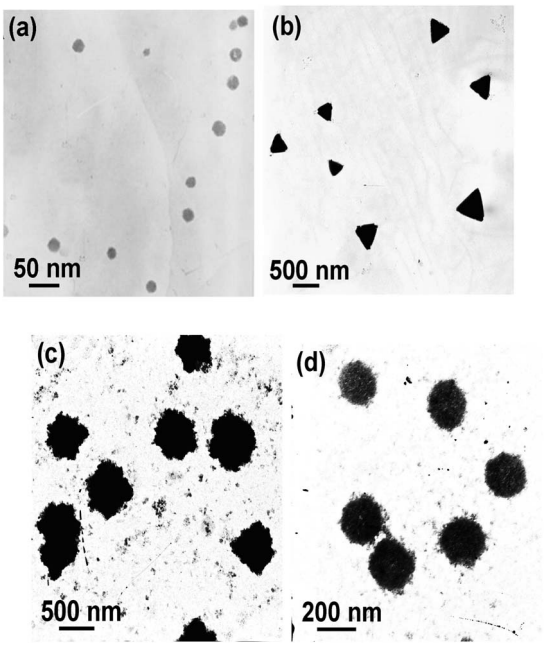

Fig. 5 TEM images of the crystalline aggregates prepared from the acidic $CuCl_2$ solutions ($[Cu^{2+}] = 38.0$ mM, $[H^+] = 18.0$ mM) with various micelle concentrations: (a) 0; (b) 0.49; (c) 0.78; (d) 1.55 g L^{-1}.

on the surface of the micelles with Cu^{2+} and H^+ in the solution play an essential role in controlling the crystalline growth process, which yields well-defined crystal structures. During the shape transition process (from sphere to triangle to sphere) we did not observe any truncated triangles, which may indicate that this is predominantly a kinetically controlled process where the triangles are indeed metastable structures.[17–19] The edge lengths of the triangular single crystalline $CuCl_2$ can be precisely controlled from a few tens of nms to a few tens of μms by adjusting the micelle/proton ratio. However, the roles of the counter ions (SO_4^{2-} or Cl^-), size/volume fraction of BCPs, temperature, and time evolutions are yet to be studied in detail in order to gain a complete understanding of the roles of kinetically and thermodynamically controlled processes.

Based on the above results, a mechanism for the formation of multiple crystal structures and the evolution of different crystalline forms is proposed as follows. According to the hard–soft acid–base theory, Cu^{2+} ions are soft Lewis acids[15,20] and have favorable mutual affinity for the sulfonic acid groups on the corona of the micelles. This ionic interaction might induce the micelles to form larger aggregates because Cu^{2+} ions can complex with two sulfonic acid groups (Fig. 2a).[21] The size and shape of the aggregates are governed by these ionic interactions. When H^+ is introduced to the solution, it competes with Cu^{2+} for the sulfonic acid groups, leading to the formation of supersaturated $CuCl_2$ particles, which function as nuclei. These particles then undergo ordered growth along the interface between the micelles and the aqueous phase due to the confinement of the polymeric micelles. Meanwhile, crystallographic registry, a process accompanied by rearrangement or desorption of the block copolymer, occurs.[14] As the concentration of H^+ increases, the growth of individual particles through

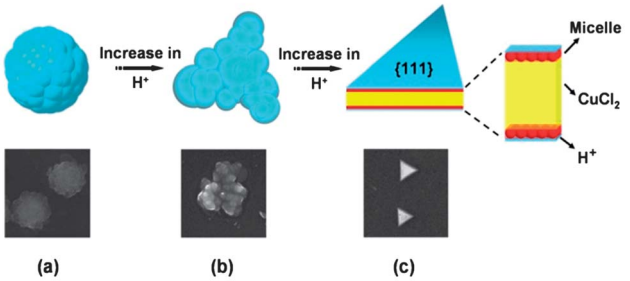

Scheme 1 Schematic representation of the formation of $CuCl_2$ (a) polycrystals, (b) mesocrystals, and (c) single crystals.

oriented aggregation is then promoted, facilitating the formation of mesocrystals as shown in Scheme 1b. The shape of the mesocrystal (triangle) is the result of spatial confinement of the micelles.[22–24] Upon further increases in the H^+ concentration, more Cu^{2+} ions contribute to the crystal growth through aggregation. The selective adsorption of micelles on the [111] facets decreases the energy of these facets and facilitates the growth of primary particles in 2D mode to produce triangular nanoplates with confined [111] planes (Scheme 1c and Fig. 2d).[9,14,21,25,26] Moreover, additional H^+ ions act as a protective agent against aggregation of the particles as well as the re-adsorption of Cu^{2+} (enlarged view of Scheme 1c).[27] In other words, two processes take place simultaneously in the system. At lower acid concentrations, there are not enough H^+ ions to compete with Cu^{2+} ions in their adsorption with the charged groups ($-SO_3H$), The increase in H^+ ions promotes the formation of $CuCl_2$ primary particles, while the PS-*b*-sPCHD micelles restrict the primary particles from disordered aggregation (precipitation) through confinement and adsorption. As a result, the growth of $CuCl_2$ particles along one direction is the dominant process in crystal formation. The unique chain conformation of sPCHD might also play a role.[9] As discussed above, the balance of the ions (H^+ to Cu^{2+} ratio) and their equilibrations with $-SO_3H$ groups, along with the spatial confinement from PS-*b*-sPCHD micelles determine this oriented mineralization process. This is consistent with other work reported in the literature.[28,29]

Our ongoing experiments show that micelles formed from another charged block copolymer (polystyrene-*block*-sulfonated polystyrene, PS-*b*-PSS) induce similar confinement effects but with different single crystal shapes, indicating that this approach can be extended to the preparation of different ordered crystal structures with a precision hard to achieve with other approaches.

In summary, we present, for the first time, the formation of $CuCl_2$ triangular nanocrystals through the confinement of charged block copolymer micelles under acidic conditions. The competition of the ionic interactions, and the polymeric confinement are believed to be the critical factors in the directional crystal growth process. The well-defined triangular morphology of the nanocrystals is a result of the interplay of these factors in this self-assembled system. The controlled mineralization presented in this work provides a model system for understanding the mechanism of biomineralization processes. It will also broaden the applications of charged polymeric micelles into other fields such as templated shape-controlled synthesis of nano- to meso-scale crystals.

Acknowledgements

This work was supported by the National Science Foundation of China (50673026, 20574018) and Doctoral Foundation of Education Ministry of China (Grant no. 20050251008), and Projects of Shanghai Municipality (B502, 06SU07002, 0652nm021, and 082231) are also acknowledged. A portion of this research was conducted at the Center for Nanophase Materials Sciences, which is sponsored at Oak Ridge National Laboratory by the Scientific User Facilities Division, Office of Basic Energy Sciences, U.S. Department of Energy.

Notes and references

1 J. E. Millstone, S. J. Hurst, G. S. Métraux, J. I. Cutler and C. A. Mirkin, *Small*, 2009, **5**, 646–664.
2 H. Jing, L. Zhang and H. Wang, in *UV-VIS and Photoluminescence Spectroscopy for Nanomaterials Characterization*, ed. C. S. S. R. Kumar, Springer, Berlin Heidelberg, 2013, pp. 1–74.
3 B. Viswanath, P. Kundu, A. Halder and N. Ravishankar, *J. Phys. Chem. C*, 2009, **113**, 16866–16883.
4 M. Ramanathan, L. K. Shrestha, T. Mori, Q. Ji, J. P. Hill and K. Ariga, *Phys. Chem. Chem. Phys.*, 2013, **15**, 10580–10611.
5 J. Koetz, J. Bahnemann, G. Lucas, B. Tiersch and S. Kosmella, *Colloids Surf., A*, 2004, **250**, 423–430.
6 J. Koetz and S. Kosmella, *Polyelectrolytes and Nanoparticles*, Springer-Verlag, Berlin, 2007.
7 A. Köth, D. Appelhans, C. Prietzel and J. Koetz, *Colloids Surf., A*, 2012, **414**, 50–56.
8 J. Koetz, M. Saric, S. Kosmella and B. Tiersch, in *Mesophases, Polymers, and Particles*, Springer, Berlin Heidelberg, 2004, pp. 95–104.
9 J. Lin, W. Ding, K. Hong, J. W. Mays, Z. Xu and Y. Yuan, *Soft Matter*, 2008, **4**, 1605–1608.
10 L. Lu, M. L. Sui and K. Lu, *Science*, 2000, **287**, 1463–1466.
11 W. Zhang, X. Wen and S. Yang, *Inorg. Chem.*, 2003, **42**, 5005–5014.
12 R. N. Briskman, *Sol. Energy Mater. Sol. Cells*, 1992, **27**, 361–368.
13 D. Malferrari, S. Fermani, P. Galletti, M. Goisis, E. Tagliavini and G. Falini, *Langmuir*, 2013, **29**, 1938–1947.
14 A. N. Kulak, P. Iddon, Y. Li, S. P. Armes, H. Cölfen, O. Paris, R. M. Wilson and F. C. Meldrum, *J. Am. Chem. Soc.*, 2007, **129**, 3729–3736.
15 A.-W. Xu, W.-F. Dong, M. Antonietti and H. Cölfen, *Adv. Funct. Mater.*, 2008, **18**, 1307–1313.
16 S.-H. Yu, H. Cölfen and M. Antonietti, *J. Phys. Chem. B*, 2003, **107**, 7396–7405.
17 X. Jiang, Q. Zeng and A. Yu, *Langmuir*, 2007, **23**, 2218–2223.
18 S. Botasini, E. Dalchiele, J. Benech and E. Méndez, *J. Nanopart. Res.*, 2011, **13**, 2819–2828.

19 O. V. Kharissova, B. I. Kharisov, T. H. García and U. O. Méndez, *Synth. React. Inorg., Met.-Org., Nano-Met. Chem.*, 2009, **39**, 662–684.
20 C. H. B. Ng and W. Y. Fan, *J. Phys. Chem. B*, 2006, **110**, 20801–20807.
21 Y. Xiong, J. M. McLellan, J. Chen, Y. Yin, Z.-Y. Li and Y. Xia, *J. Am. Chem. Soc.*, 2005, **127**, 17118–17127.
22 Z. Ou and M. Muthukumar, *J. Chem. Phys.*, 2005, **123**, 074905.
23 Z. Ou and M. Muthukumar, *J. Chem. Phys.*, 2006, **124**, 154902.
24 M. Ramanathan, S. M. Kilbey II, Q. Ji, J. P. Hill and K. Ariga, *J. Mater. Chem.*, 2012, **22**, 10389–10405.
25 I. Washio, Y. Xiong, Y. Yin and Y. Xia, *Adv. Mater.*, 2006, **18**, 1745–1749.
26 Y. Xiong, I. Washio, J. Chen, H. Cai, Z.-Y. Li and Y. Xia, *Langmuir*, 2006, **22**, 8563–8570.
27 E. M. Pouget, P. H. H. Bomans, J. A. C. M. Goos, P. M. Frederik, G. de With and N. A. J. M. Sommerdijk, *Science*, 2009, **323**, 1455–1458.
28 S. Cavalli, D. C. Popescu, E. E. Tellers, M. R. J. Vos, B. P. Pichon, M. Overhand, H. Rapaport, N. A. J. M. Sommerdijk and A. Kros, *Angew. Chem., Int. Ed.*, 2006, **45**, 739–744.
29 E. Leontidis, T. Kyprianidou-Leodidou, W. Caseri and K. C. Kyriacou, *Langmuir*, 1999, **15**, 3381–3385.

